RESEARCH FRONT

CSIRO PUBLISHING

Full Paper

Aust. J. Chem.
http://dx.doi.org/10.1071/CH15650

Hybrid 1,2,3-Triazole Supported Cu^{II} Complexes: Tuning Assembly and Weak Interaction-Driven Crystal Growth

Shi-Qiang Bai,[A,D] *Lu Jiang,*[A] *David James Young,*[A,B] *and T. S. Andy Hor*[A,C]

[A]Institute of Materials Research and Engineering, A*STAR (Agency for Science, Technology and Research), 2 Fusionopolis Way, #08-03, Innovis, Singapore 138634, Republic of Singapore.
[B]Faculty of Science, Health, Education and Engineering, University of the Sunshine Coast, Maroochydore DC, Qld 4558, Australia.
[C]Department of Chemistry, National University of Singapore, 3 Science Drive 3, Singapore 117543, Republic of Singapore.
[D]Corresponding author. Email: bais@imre.a-star.edu.sg

Two new dinuclear Cu^{II} complexes $[Cu_2Cl_4(L1)_2]$ (**1**) and $[Cu_2Cl_4(L2)_2]$ (**2**) (L1 = 2-((4-(2-(cyclopentylthio)ethyl)-1*H*-1,2,3-triazol-1-yl)methyl)pyridine; L2 = 2-((4-(pyridin-2-yl)-1*H*-1,2,3-triazol-1-yl)methyl)benzonitrile) were synthesised and characterised by single-crystal X-ray diffraction (XRD), powder XRD, thermogravimetric analysis, elemental analysis and IR measurements. The picolyl-triazole ligand L1 coordinates in a chelate-bridging mode forming a dinuclear structure **1**. The more rigid pyridyl-triazole ligand L2 chelates only, generating a chloride-bridged dinuclear complex **2**. Both crystals of complexes **1** and **2** show dominant plate shapes that correlate with weak 2D H-bonding interactions in the lattice. A mononuclear structure (**3**, $[CuCl_2(L3)_2]\cdot 6H_2O$, L3 = 3-((4-(pyridin-2-yl)-1*H*-1,2,3-triazol-1-yl)methyl)benzonitrile) yields block shape crystals that correlate with 3D H-bonding interactions. This study demonstrates tunable assembly at the molecular level and the relationship of crystal shape with weak lattice interactions.

Manuscript received: 15 October 2015.
Manuscript accepted: 4 November 2015.
Published online: 14 December 2015.

Introduction

Organic–inorganic hybrid materials exhibit fascinating structures, tunable properties and have potential applications in catalysis, magnetism and as biomimetic materials.[1–5] Metal complexes formed from organic ligands and metal centres are particularly attractive due to their well defined structures and multifunctional properties.[6–10] A variety of organic ligands with different metal ions have been used in the synthesis of novel metal complexes.[11–15] However, the predictable preparation of targeted materials is still a challenge. Design and control is possible by manipulation of ligand structure and choice of metal ion, anion, cation, solvent and temperature. Single-crystal X-ray diffraction (XRD) technology is fundamental to this science, providing precise lattice structures and crystal face information. This technique, therefore, permits the correlation of crystal shape with molecular characteristics. Establishing this relationship can assist in the controlled synthesis of functional materials and this is our current focus.[16–18] Our ligands of choice for this investigation are the functionalised 1,2,3-triazoles, obtained from copper-catalysed azide–alkyne cycloaddition ('click reactions') (CuAAC).[19–22] This reliable reaction can provide ligands with a variety of precisely oriented donor atoms.[23–28] Some formation trends and tunable properties have been discovered in these studies. We recently observed, for example, that the long axis (dominant growth direction) of a prism crystal can be driven by weak one-dimensional $\pi\cdots\pi$ stacking interactions in the lattice.[29] In the present work, we expand this study with three hybridised 1,2,3-triazole Cu^{II} complexes (Chart 1), correlating their molecular structures and lattice interactions with crystal shape.

Results and Discussion

Synthesis and Characterisation

Ligands L1–L3 were synthesised from one-pot CuAAC reactions. The Cu^{II} complexes **1–3** were prepared by the reaction of the corresponding ligand L1, L2, or L3 with $CuCl_2$ in CH_3OH. The bulk single crystals of both **1** and **2** are dominant plates while the single crystals of **3** are block shaped. Powder samples were collected by filtration under vacuum and washed with CH_3OH and diethyl ether. The identity and purity of the crystal and powder samples of complexes **1** and **2** were confirmed by single-crystal and powder XRD measurements (Fig. 1) together with microanalysis. The infrared spectrum of complex **2** displayed a characteristic vibration for the C≡N bond at 2227 cm^{-1}. Complexes **1** and **2** were thermally stable up to ~160 and 220°C in air, respectively, followed by steady declines until reaching residual weights at ~680°C (Fig. 2).

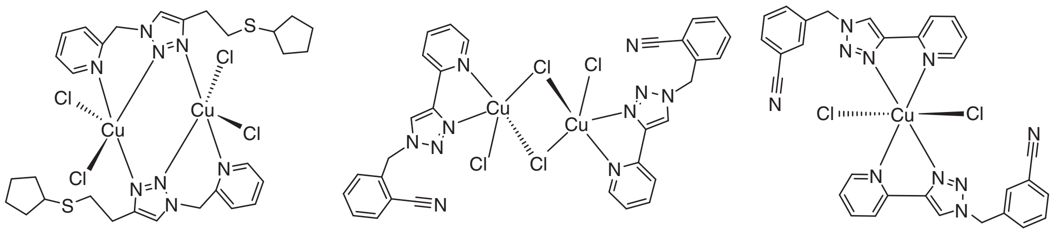

1 2 3

Chart 1. The coordination modes of ligands L1–L3 in Cu^{II} complexes **1–3**.

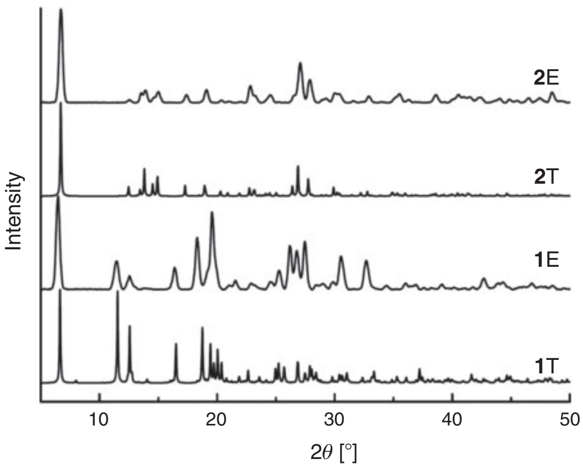

Fig. 1. Powder XRD patterns of **1** and **2** (T = theoretical profile referenced to the experimentally determined single-crystal XRD pattern; E = experimental data).

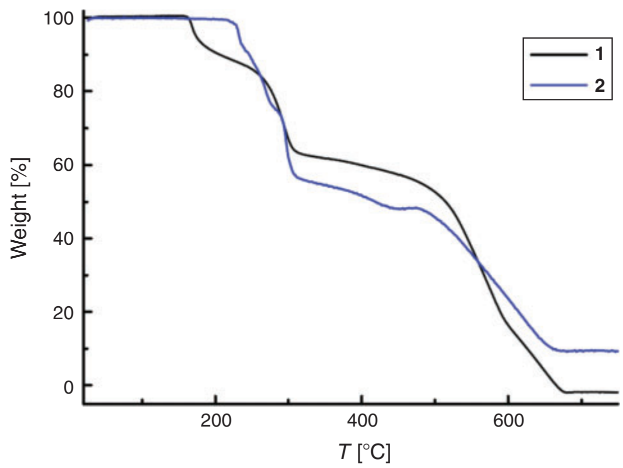

Fig. 2. TGA curves of **1** and **2**.

Molecular Structures

Complex **1** crystallises in the monoclinic crystal system with a space group of $P2_1/c$. It consists of discrete neutral and asymmetric dinulear Cu^{II} units (Fig. 3a). The Cu^{II} centres can be viewed as five-coordinated in distorted square pyramidal geometries with an Addison parameter (τ) of ~0.33 for both Cu1 and Cu2.[30] Each square base consists of two *trans* nitrogen atoms (N1 and N8 for Cu1, N4 and N5 for Cu2) from two L1 ligands, and two *trans* orientated chloride ligands. The apical positions are occupied by the 2′-$N_{Triazole}$ nitrogen atoms (N3 and N7) with long Cu–N bonds (2.61 and 2.59 Å), respectively. The triazolyl N=N bridges therefore present in an asymmetric basal-apical fashion between two Cu^{II} centres. The torsion angles between the two Cu atoms along the Cu–N=N–Cu moiety are 111.8° and 72.6°, respectively. Deviations of both Cu^{II} centres from the mean planes of the square bases (N1–N8–Cl1–Cl2 and N4–N5–Cl3–Cl4) are similar (~0.20 Å). Weak intermolecular H-bonding interactions exist in the lattice between the L1 skeleton and the chloride ligands, forming a two-dimensional supramolecular layer in the *ab* plane (Fig. 3b,c, Table 1), aligned with the dominant crystal face (*ab*) (Fig. 3d). The neighbouring layers are symmetrically packed along the *c* direction. The intra- and intermolecular Cu···Cu distances are 4.42 and 7.60 Å, respectively.

Complex **2** crystallises in the triclinic crystal system with a space group of $P-1$. It consists of discrete neutral and symmetric chloride-bridged dinuclear Cu^{II} units (Fig. 4a). The Cu^{II} centre can be viewed as a five-coordinated distorted square pyramidal geometry with an Addison parameter (τ) of 0.05.[30] The square base of the pyramid consists of two *cis* nitrogen atoms (N1 and N4) of one L2 ligand, and two *cis* orientated chloride ligands. The apical position is occupied by the chloride ligand (Cl2A) with a long Cu–Cl bond (2.77 Å). The bridging angle is ~88.1°. The deviation of the Cu^{II} centre from the mean plane of the square base (N1–N4–Cl1–Cl2) is about ~0.16 Å. There are also weak intermolecular H-bonding interactions between the L2 skeleton and the chloride ligands and π···π stacking between the triazole and pyridine rings (centroid–centroid distance 3.84 Å), which synergistically drive the formation of a 2D supramolecular layer in the *ab* plane (Fig. 4b, c, Table 1) aligned with the crystal face (Fig. 4d, e). The neighbouring layers are packed along the *c* direction. The intra- and intermolecular Cu···Cu distances are 3.52 and 5.44 Å, respectively.

Complex **3** crystallises in the monoclinic crystal system with a space group of $P2_1/n$. It consists of discrete neutral and symmetric mononulear Cu^{II} units (Fig. 5a). The Cu^{II} centre can be viewed as six-coordinate in distorted octahedral geometry formed from four nitrogen atoms (N1, N4, N1A, and N4A) of two chelating L3 ligands and two *trans* orientated chloride ligands. Although L2 and L3 exhibit similar chelating coordination modes in **2** and **3**, the chloride ligands are *cis* in **2** and *trans* in **3**. Moreover, intramolecular C–H···N interactions, cyclic H-bonding interactions among lattice water molecules and coordinated chloride ligands (Fig. 5b, Table 1), lattice water molecules that H-bond to ligand L3, and additional L3···L3 and L3···Cl H-bonding create a 3D supramolecular structure (Fig. 5c, Table 1) that aligns with the block shape of the single crystal (Fig. 5d).

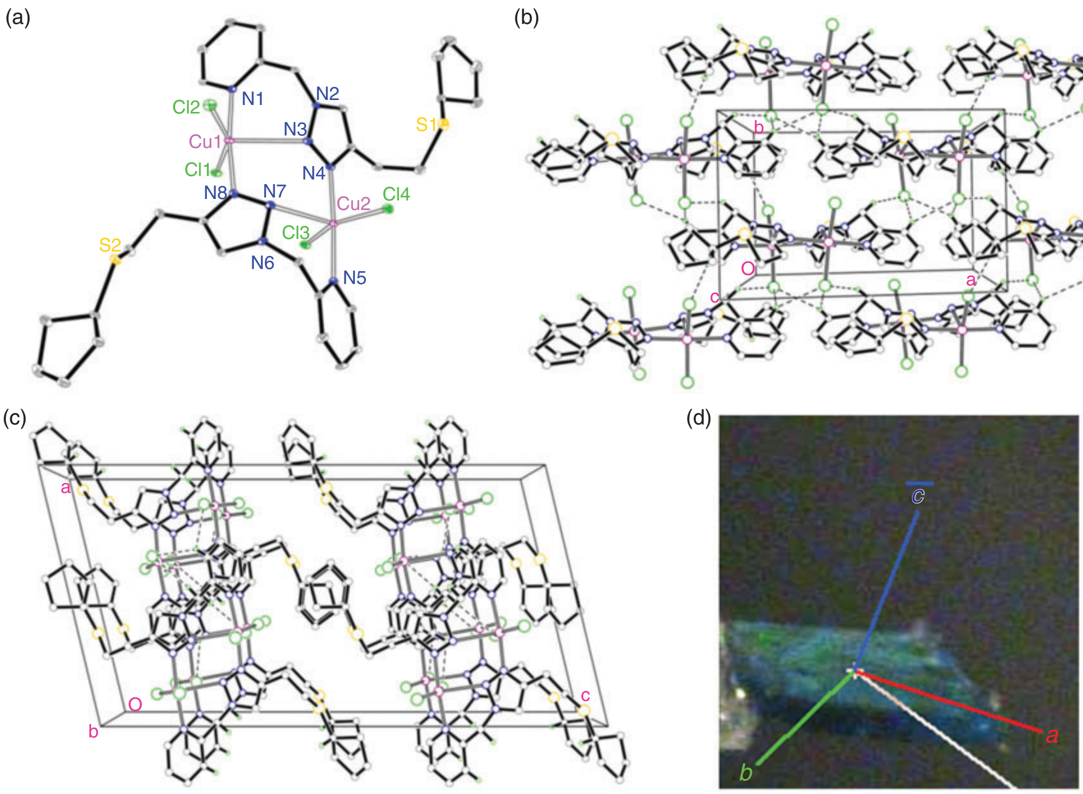

Fig. 3. (a) Molecular structure of **1**. (b) 2D hydrogen-bonding interactions in **1**. (c) The packing structure of **1**. (d) A single-crystal image of **1** with lattice directions.

Table 1. Hydrogen-bond parameters in complexes 1–3

D–H···A	D–H [Å]	D···A [Å]	H···A [Å]	∠D–H···A [°]
Complex **1**				
C4–H···Cl3^{A}	0.95	3.378(4)	2.77	123
C6–H···Cl1^{A}	0.99	3.527(3)	2.61	155
C19–H···Cl1^{B}	0.95	3.430(4)	2.76	129
C21–H···Cl3^{B}	0.99	3.561(3)	2.70	146
C26–H···Cl4^{C}	1.00	3.655(4)	2.66	172
Symmetry codes: $^{A}1-x, y-0.5, 0.5-z$; $^{B}-x, y-0.5, 0.5-z$; $^{C}-x, y+0.5, 0.5-z$.				
Complex **2**				
C4–H···Cl2^{A}	0.93	3.652(4)	2.77	160
C7–H···Cl2^{A}	0.93	3.573(3)	2.72	152
C8–H···Cl1^{A}	0.97	3.618(3)	2.72	155
Symmetry code: $^{A}x-1, y-1, z$.				
Complex **3**				
C1–H···N3^{A}	0.93	3.170(2)	2.38	143
C2–H···N5^{B}	0.93	3.399(2)	2.55	151
C7–H···O1^{C}	0.93	3.428(3)	2.58	152
C8–H···Cl1^{D}	0.97	3.703(2)	2.83	150
C14–H···O3^{E}	0.93	3.368(3)	2.49	157
O1–H···Cl1^{F}	0.84	3.177(2)	2.41	152
O1–H···O2	0.85	2.715(3)	2.43	100
O2–H···Cl1^{A}	0.84	3.259(3)	2.47	158
O2–H···O3	0.84	2.832(3)	2.02	163
O3–H···N5^{D}	0.84	3.019(3)	2.20	164
O3–H···O1^{G}	0.84	2.767(3)	1.93	171
Symmetry codes: $^{A}1-x, 1-y, -z$; $^{B}1+x, y-1, z$; $^{C}1+x, y, z$; $^{D}0.5+x, 1.5-y, 0.5+z$; $^{E}0.5-x, 0.5+y, 0.5-z$; $^{F}x-0.5, 1.5-y, 0.5+z$; $^{G}0.5-x, y-0.5, 0.5-z$.				

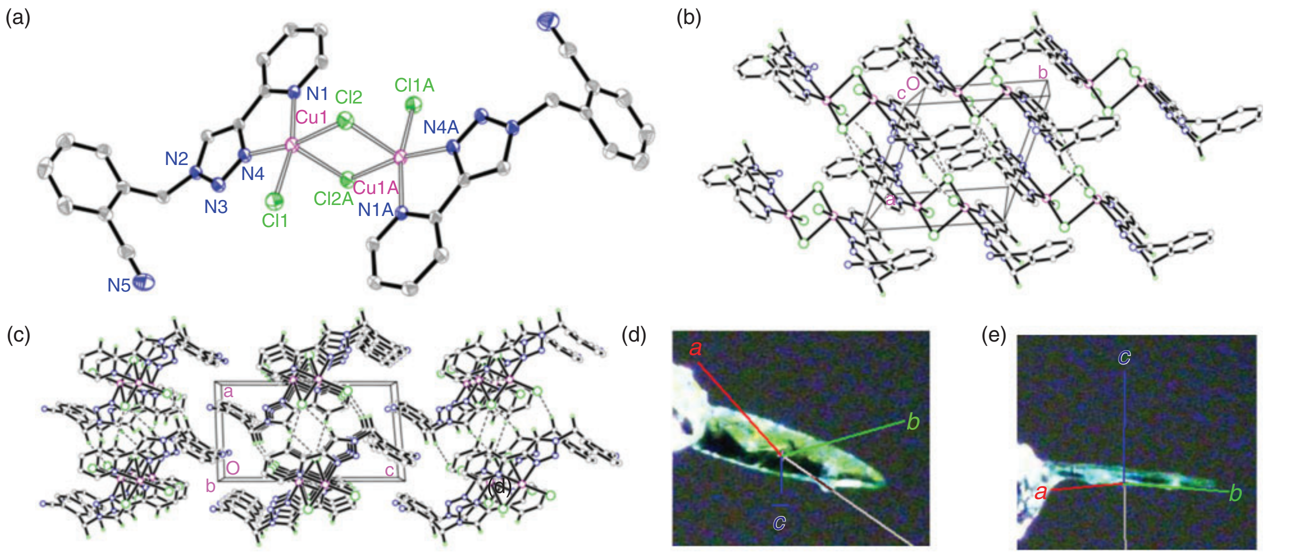

Fig. 4. (a) Molecular structure of **2**. (b) 2D hydrogen-bonding interactions in **2**. (c) The packing structure of **2**. (d, e) Single-crystal images of **2** with lattice directions in different orientations.

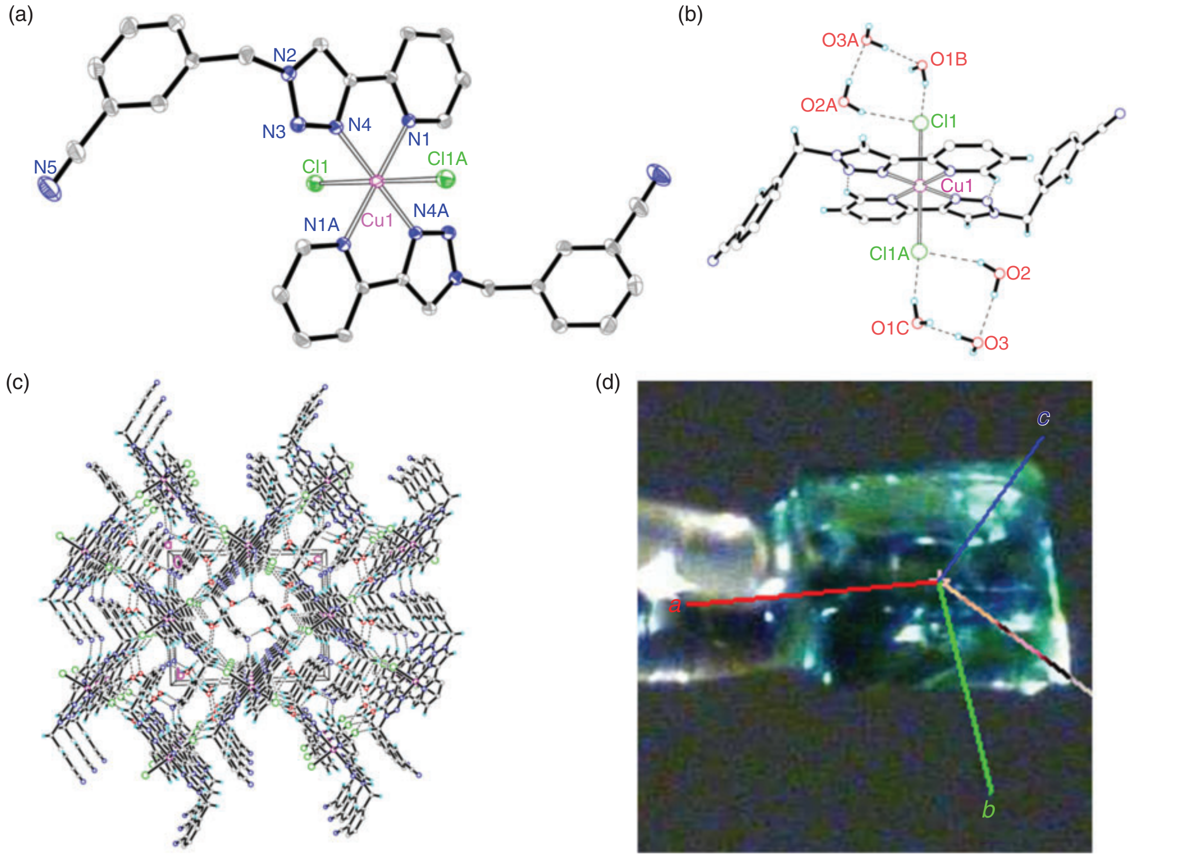

Fig. 5. (a) Molecular structure of **3**. (b) Cyclic H-bonding structures and intramolecular C–H···N H-bonding interactions in **3**. (c) The packing structure of **3** (only the H-bonding associated H atoms were kept for clarity). (d) A single-crystal image of **3** with lattice directions.

Structural Relationships

Most attention in the fields of single-crystal crystallography, crystal engineering, and crystal growth and design has concentrated on structure, properties, and potential applications. The weak interaction responsible for crystal morphology is a comparatively neglected field of investigation. We are curious about how the dominant growth direction of a crystal is related to weak lattice interactions. In this work, the flexible ligand L1 provides the chelate-bridging mode in the ligand bridged dinuclear structure **1** while the more rigid L2 simply chelates and forms a di-chloride bridged structure **2**. Both of these crystals are dominant plates and the crystal faces in the *ab* plane

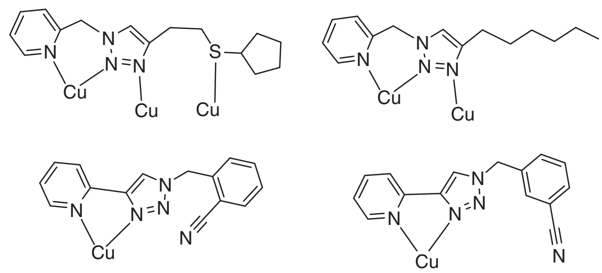

Chart 2. Coordination modes of triazole $Cu^{I/II}$ complexes.

are aligned with the lattice H-bonding interactions in the *ab* plane. There are no obvious intermolecular interactions between the *ab* planes, which therefore limits growth in the *c* dimension of the single crystals. Ligand L3 yields a mononuclear complex **3** with octahedron geometry and block crystal shape. We propose that its 3D H-bonding lattice interactions drive bulk crystal formation towards this block shape.

Ligand L1 has the potential for both N and S coordination to Cu^{I} (Chart 2).[16] In the present study, the flexible S substituent is pending and the ligand adopts a chelate-bridging mode of coordination similar to that of our previously reported (1-(2-picolyl)-4-hexyl-1*H*-1,2,3-triazole) ligand which also has a flexible substituent and similarly supports a dinuclear Cu^{II} complex.[28] By comparison, the more rigid L2 does not bridge the Cu^{II} centres. Although both L2 and L3 prefer this chelating mode of coordination to $Cu^{II/I}$ (Chart 2),[29] the CN substituent group at the slightly more remote 3′ position provides greater opportunity for water molecules and other donors to access the Cu^{II} centre (6 donors in **3** and 5 in **2**). Lattice molecules, such as water or solvent molecules, are difficult to predict or control. They can, however, influence the intermolecular interactions and the growth of the crystal. A comparison of complexes **2** and **3** provides some clues in this respect.

Conclusion

The current work provides an experimental model for further probing the relationship between crystal shape (dominant growth dimensions) and weak intermolecular forces. These forces can be between molecular backbones and/or with solvent molecules. These interactions are tunable with structure, potentially permitting predictable control of crystal morphology.

Experimental

General

Sodium azide is potentially explosive. Only micro-scale reactions are advisable and all operations must be performed with necessary precautions. All starting chemicals were used as received. Elemental analyses were performed on a Thermo Electron Corporation Flash EA 1112 series analyser. Infrared spectra were obtained on a Perkin Elmer Spectrum 2000 FT-IR spectrometer from samples in KBr discs. Electrospray ionisation mass spectra (ESI-MS) for L2 were recorded in positive ion mode using a Shimadzu LCMS-IT-TOF mass spectrometer. Powder XRD data were collected on a Bruker AXS GADDS X-ray diffractometer with Cu-Kα radiation (λ 1.54056 Å). Thermogravimetric analyses (TGA) were carried out in an air stream using a TA Instruments TGA Q500 analyser with a heating rate of 20°C min^{-1}.

Synthesis

Ligands L1 and L3 were synthesised according to recent reports.[16,29] Ligand L2 can be synthesised using a similar method to that for L3. In a typical procedure for L2, 2-(bromomethyl)benzonitrile (392 mg, 2 mmol), NaN_3 (143 mg, 2.2 mmol), 2-ethynylpyridine (258 mg, 2.5 mmol), and CuI (23 mg, 0.12 mmol) were placed in a reaction tube containing a mixed solvent of CH_3OH/H_2O (1 : 1, 4 mL). The reaction was stirred at 50°C for 24 h on a MultiMax reactor and then extracted three times with ethyl acetate. The combined organic extracts were washed with brine, concentrated, and purified by column chromatography on silica.

2-((4-(Pyridin-2-yl)-1H-1,2,3-triazol-1-yl)methyl) benzonitrile (L2)

Formula weight: $C_{15}H_{11}N_5$, 261.29. Yield: ~500 mg, 95 %. *m/z* 262 (100 %, $[L2 + H]^+$), 284 (12, $[L2 + Na]^+$). δ_H ($CDCl_3$, 500.2 MHz) 8.54 (s, 1H), 8.24 (s, 1H), 8.16 and 8.14 (d, 1H, *J* 8), 7.77, 7.76 and 7.74 (t, 1H, *J* 8), 7.71 and 7.70 (d, 1H, *J* 8), 7.59, 7.57 and 7.56 (t, 1H, *J* 7), 7.46, 7.45 and 7.44 (t, 1H, *J* 7), 7.36 and 7.35 (d, 1H, *J* 8), 7.21 (s, 1H), 5.81 (s, 2H, CH_2). δ_C ($CDCl_3$, 125.8 MHz) 149.9, 149.4, 149.0, 138.0, 137.2, 133.8, 133.2, 129.54, 129.48, 123.1, 122.6, 120.4, 116.9, 112.1 (pyridyl, triazole and CN groups), 51.9 (CH_2) (for spectra, see the Supplementary Material).

*$[Cu_2Cl_4(L1)_2]$ (**1**)*

A CH_3OH solution (5 mL) of $CuCl_2 \cdot 2H_2O$ (0.1 mmol, 17 mg) was added into a CH_3OH solution (5 mL) of ligand L1 (0.1 mmol, 29 mg) in a vial with stirring. The mixture was filtered and slow evaporation of the resulting solution afforded blue crystals of **1** within two weeks. Yield: 23 mg, 54 %. Anal. Calc. for $C_{15}H_{20}Cl_2CuN_4S$ (422.85): C 42.61, H 4.77, N 13.25. Found: C 42.57, H 4.82, N 13.36 %. ν_{max} /cm^{-1} 3134m, 3074m, 2995m, 2958m, 2866m, 1606m, 1572m, 1549m, 1482m, 1434m, 1368m, 1344m, 1324m, 1304m, 1282m, 1228m, 1172m, 1155m, 1103m, 1073m, 1025m, 841m, 813m, 772s, 727m, 674m, 646m, 632m, 434m.

*$[Cu_2Cl_4(L2)_2]$ (**2**)*

Green crystals of complex **2** were prepared using the procedure described above for complex **1** by replacing L1 with L2. Yield: 28 mg, 71 %. Anal. Calc. for $C_{15}H_{11}Cl_2CuN_5$ (395.73): C 45.53, H 2.80, N 17.70. Found: C 44.99, H 3.12, N 17.03 %. ν_{max} /cm^{-1} 3088m, 3000m, 2951m, 2227m ($\nu_{C\equiv N}$), 1618m, 1579m, 1494m, 1469m, 1454m, 1366m, 1339m, 1279m, 1249m, 1217m, 1161m, 1117m, 1094m, 1052m, 1019m, 997m, 897m, 854m, 835m, 783m, 765s, 743m, 704m, 689m, 644m, 602m, 555m, 514m, 417m.

Table 2. Summary of crystallographic data for 1–3

Parameter	1	2	3
Formula	$C_{30}H_{40}Cl_4Cu_2N_8S_2$	$C_{30}H_{22}Cl_4Cu_2N_{10}$	$C_{30}H_{34}Cl_2CuN_{10}O_6$
M_W	845.70	791.46	765.11
T/K	100(2)	296(2)	296(2)
Crystal size [mm^3]	0.32 × 0.24 × 0.05	0.41 × 0.08 × 0.02	0.30 × 0.22 × 0.17
Crystal system	Monoclinic	Triclinic	Monoclinic
Space group	$P\,2_1/c$	$P{-}1$	$P\,2_1/n$
a [Å]	14.5067(8)	7.7217(9)	9.1207(3)
b [Å]	9.1277(5)	8.202(1)	12.4895(4)
c [Å]	27.312(1)	13.196(2)	15.6002(5)
α [°]	90	92.736(3)	90
β [°]	103.490(1)	92.077(3)	106.203(1)
γ [°]	90	113.073(3)	90
V [Å^3]	3516.7(3)	766.7(2)	1706.5(1)
Z	4	1	2
D_{calc} [g cm^{-3}]	1.597	1.714	1.489
μ [mm^{-1}]	1.668	1.777	0.855
θ range [°]	1.44–26.40	1.55–23.81	2.12–33.16
Reflections collected	41723	15260	51775
Independent reflections [R_{int}]	6876 [0.0388]	2266 [0.0441]	6496 [0.0289]
Parameters	415	208	241
GOF	1.084	1.063	1.032
$R_1(I>2\sigma(I))$	0.0412	0.0307	0.0329
wR_2(all data)	0.0877	0.0833	0.0974

*[$CuCl_2(L3)_2$]·$6H_2O$ (**3**)*

Green crystals of complex **3** were prepared using the procedure described above for complex **1** by replacing L1 with L3. Only single-crystal XRD measurements were performed due to limited sample amount.

X-Ray Diffraction

The single-crystal XRD data were collected using a Bruker AXS SMART APEXII CCD diffractometer using $Mo_{K\alpha}$ radiation (λ 0.71073 Å) (Table 2). Data integration and scaling were performed using Bruker *SAINT*.[31] The empirical absorption correction was performed by *SADABS*.[32] The space group determination, structure solution, and least-squares refinements on $|F|^2$ were carried out using Bruker *SHELXL*.[33] The structures were solved by direct methods to locate the heavy atoms, followed by difference maps for the light non-hydrogen atoms. Anisotropic thermal parameters were refined for the rest of the non-hydrogen atoms. Hydrogen atoms were placed geometrically and refined isotropically. For complex **3**, hydrogen atoms H1–H6 were located from a difference map, the positions were refined with DFIX constraints for O–H and H···H of water, with a thermal parameter at −1.2000. CCDC reference numbers are: 1431197 (**1**), 1431198 (**2**), 1431199 (**3**).

Supplementary Material

The ^{1}H and ^{13}C NMR spectra of ligand L2 are available on the Journal's website.

Acknowledgements

The authors gratefully acknowledge the financial support (IMRE/14-1C0248, IMRE/15-1C0202, SERC Grant No. 1527200020) of the Institute of Materials Research and Engineering, A*STAR, and the National University of Singapore.

References

[1] J.-N. Rebilly, B. Colasson, O. Bistri, D. Over, O. Reinaud, *Chem. Soc. Rev.* **2015**, *44*, 467. doi:10.1039/C4CS00211C

[2] P. Silva, S. M. F. Vilela, J. P. C. Tomé, F. A. A. Paz, *Chem. Soc. Rev.* **2015**, *44*, 6774. doi:10.1039/C5CS00307E

[3] A. Kaushik, R. Kumar, S. K. Arya, M. Nair, B. D. Malhotra, S. Bhansali, *Chem. Rev.* **2015**, *115*, 4571. doi:10.1021/CR400659H

[4] A. B. Descalzo, R. Martínez-Máñez, F. Sancenón, K. Hoffmann, K. Rurack, *Angew. Chem. Int. Ed.* **2006**, *45*, 5924. doi:10.1002/ANIE.200600734

[5] L. D. Carlos, R. A. S. Ferreira, V. de Zea Bermudez, S. J. L. Ribeiro, *Adv. Mater.* **2009**, *21*, 509. doi:10.1002/ADMA.200801635

[6] H. Schmidbaur, A. Schier, *Angew. Chem. Int. Ed.* **2015**, *54*, 746. doi:10.1002/ANIE.201405936

[7] M. Iglesias, A. Iturmendi, P. J. S. Miguel, V. Polo, J. J. Pérez-Torrente, L. A. Oro, *Chem. Commun.* **2015**, *51*, 12431. doi:10.1039/C5CC04287A

[8] C. B. Aakeröy, A. M. Beatty, D. S. Leinen, *Angew. Chem. Int. Ed.* **1999**, *38*, 1815. doi:10.1002/(SICI)1521-3773(19990614)38:12<1815::AID-ANIE1815>3.0.CO;2-S

[9] J. D. Crowley, P. H. Bandeen, *Dalton Trans.* **2010**, *39*, 612. doi:10.1039/B911276F

[10] Y. Chen, H.-X. Li, D. Liu, L.-L. Liu, N.-Y. Li, H.-Y. Ye, Y. Zhang, J.-P. Lang, *Cryst. Growth Des.* **2008**, *8*, 3810. doi:10.1021/CG8004568

[11] F. A. Almeida Paz, J. Klinowski, S. M. F. Vilela, J. P. C. Tomé, J. A. S. Cavaleiro, J. Rocha, *Chem. Soc. Rev.* **2012**, *41*, 1088. doi:10.1039/C1CS15055C

[12] M. D. Ward, P. R. Raithby, *Chem. Soc. Rev.* **2013**, *42*, 1619. doi:10.1039/C2CS35123D

[13] H. Li, Z.-J. Yao, D. Liu, G.-X. Jin, *Coord. Chem. Rev.* **2015**, *293–294*, 139. doi:10.1016/J.CCR.2014.08.014

[14] S.-Q. Bai, C.-J. Fang, Z. He, E.-Q. Gao, C.-H. Yan, T. S. A. Hor, *Dalton Trans.* **2012**, *41*, 13379. doi:10.1039/C2DT31186K

[15] N. Zhang, J.-Y. Zhang, Q.-X. Jia, W. Deng, E.-Q. Gao, *RSC Advances* **2015**, *5*, 70772. doi:10.1039/C5RA10459A

[16] S.-Q. Bai, L. Jiang, A. L. Tan, S. C. Yeo, D. J. Young, T. S. A. Hor, *Inorg. Chem. Front.* **2015**, *2*, 1011. doi:10.1039/C5QI00030K

[17] S.-Q. Bai, L. Jiang, D. J. Young, T. S. A. Hor, *Dalton Trans.* **2015**, *44*, 6075. doi:10.1039/C4DT03648D

[18] S.-Q. Bai, L. Jiang, B. Sun, D. J. Young, T. S. A. Hor, *CrystEngComm* **2015**, *17*, 3305. doi:10.1039/C4CE02282C

[19] V. V. Rostovtsev, L. G. Green, V. V. Fokin, K. B. Sharpless, *Angew. Chem. Int. Ed.* **2002**, *41*, 2596. doi:10.1002/1521-3773(20020715)41:14<2596::AID-ANIE2596>3.0.CO;2-4

[20] C. W. Tornøe, C. Christensen, M. Meldal, *J. Org. Chem.* **2002**, *67*, 3057. doi:10.1021/JO011148J

[21] M. Meldal, C. W. Tornøe, *Chem. Rev.* **2008**, *108*, 2952. doi:10.1021/CR0783479

[22] J. E. Hein, V. V. Fokin, *Chem. Soc. Rev.* **2010**, *39*, 1302. doi:10.1039/B904091A

[23] S.-Q. Bai, J. Y. Kwang, L. L. Koh, D. J. Young, T. S. A. Hor, *Dalton Trans.* **2010**, *39*, 2631. doi:10.1039/B918223C

[24] S.-Q. Bai, A. M. Yong, J. J. Hu, D. J. Young, X. Zhang, Y. Zong, J. Xu, J.-L. Zuo, T. S. A. Hor, *CrystEngComm* **2012**, *14*, 961. doi:10.1039/C1CE05808H

[25] S.-Q. Bai, L. Jiang, J.-L. Zuo, T. S. A. Hor, *Dalton Trans.* **2013**, *42*, 11319. doi:10.1039/C3DT50247C

[26] L. Jiang, Z. Wang, S.-Q. Bai, T. S. A. Hor, *Dalton Trans.* **2013**, *42*, 9437. doi:10.1039/C3DT50987G

[27] L. Jiang, Z. Wang, S.-Q. Bai, T. S. A. Hor, *CrystEngComm* **2013**, *15*, 10451. doi:10.1039/C3CE41385C

[28] S.-Q. Bai, L. Jiang, J.-L. Zuo, C.-H. Yan, T. S. A. Hor, *Aust. J. Chem.* **2013**, *66*, 1029. doi:10.1071/CH13224

[29] S.-Q. Bai, D. Kai, K. L. Ke, M. Lin, L. Jiang, Y. Jiang, D. J. Young, X. J. Loh, X. Li, T. S. A. Hor, *ChemPlusChem* **2015**, *80*, 1235. doi:10.1002/CPLU.201500202

[30] A. W. Addison, T. N. Rao, J. Reedijk, J. van Rijn, G. C. Verschoor, *J. Chem. Soc., Dalton Trans.* **1984**, 1349. doi:10.1039/DT9840001349

[31] *SAINT Software Reference Manual Version 6.0* 2003 (Bruker AXS Inc.: Madison, WI).

[32] L. Krause, R. Herbst-Irmer, G. M. Sheldrick, D. Stalke, *J. Appl. Cryst.* **2015**, *48*, 3. doi:10.1107/S1600576714022985

[33] G. M. Sheldrick, *Acta Crystallogr. Sect. C: Struct. Chem.* **2015**, *C71*, 3. doi:10.1107/S2053229614024218